### Title

An Allometric Analysis of Sex and Sex Chromosome Dosage Effects on Subcortical Anatomy in Humans




### Journal

Journal of Neuroscience, 36(8)

### ISSN

0270-6474



### Authors

Reardon, Paul Kirkpatrick
Clasen, Liv
Giedd, Jay N
et al.



### Publication Date

2016-02-24

### DOI

10.1523/jneurosci.3195-15.2016

Peer reviewed

Development/Plasticity/Repair

# An Allometric Analysis of Sex and Sex Chromosome Dosage Effects on Subcortical Anatomy in Humans

**Paul Kirkpatrick Reardon,[1] Liv Clasen,[1] Jay N. Giedd,[2] Jonathan Blumenthal,[1] Jason P. Lerch,[3] M. Mallar Chakravarty,[4,5] and Armin Raznahan[1]**

[1]Developmental Neurogenomics Unit, Child Psychiatry Branch, National Institute of Mental Health, National Institutes of Health, Bethesda, Maryland 20892, [2]Department of Psychiatry, University of California San Diego, San Diego, California 92093, [3]Department of Psychiatry and Institute of Biomaterials and Biomedical Engineering, University of Toronto, Toronto, Ontario M5T 1R8, Canada, [4]Computational Brain Anatomy Laboratory, Cerebral Imaging Centre, Douglas Mental Health University Institute, Montreal, Quebec H4H 1R3, Canada, and [5]Departments of Psychiatry and Biomedical Engineering, McGill University, Montreal, Quebec H3A 1A1, Canada

**Structural neuroimaging of humans with typical and atypical sex-chromosome complements has established the marked influence of both Yand X-/Y-chromosome dosage on total brain volume (TBV) and identified potential cortical substrates for the psychiatric phenotypes associated with sex-chromosome aneuploidy (SCA). Here, in a cohort of 354 humans with varying karyotypes (XX, XY, XXX, XXY, XYY, XXYY, XXXXY), we investigate sex and SCA effects on subcortical size and shape; focusing on the striatum, pallidum and thalamus. We find large effect-size differences in the volume and shape of all three structures as a function of sex and SCA. We correct for TBV effects with a novel allometric method harnessing normative scaling rules for subcortical size and shape in humans, which we derive here for the first time. We show that all three subcortical volumes scale sublinearly with TBV among healthy humans, mirroring known relationships between subcortical volume and TBV among species. Traditional TBV correction methods assume linear scaling and can therefore invert or exaggerate sex and SCA effects on subcortical anatomy. Allometric analysis restricts sex-differences to: (1) greater pallidal volume (PV) in males, and (2) relative caudate head expansion and ventral striatum contraction in females. Allometric analysis of SCA reveals that supernumerary X- and Y-chromosomes both cause disproportionate reductions in PV, and coordinated deformations of striatopallidal shape. Our study provides a novel understanding of sex and sex-chromosome dosage effects on subcortical organization, using an allometric approach that can be generalized to other basic and clinical structural neuroimaging settings.**

*Key words:* **allometry; aneuploidy; morphometry; sex; subcortex**

**Significance Statement**

**Sex and sex-chromosome dosage (SCD) are known to modulate human brain size and cortical anatomy, but very little is known regarding their impact on subcortical structures that work with the cortex to subserve a range of behaviors in health and disease. Moreover, regional brain allometry (nonlinear scaling) poses largely unaddressed methodological and theoretical challenges for such research. We build the first set of allometric norms for global and regional subcortical anatomy, and use these to dissect out the complex, distributed and topologically organized patterns of areal contraction and expansion, which characterize sex and SCD effects on subcortical anatomy. Our data inform basic research into the patterning of neuroanatomical variation, and the clinical neuroscience of sex-chromosome aneuploidy.**

## Introduction

Humans display replicable sex-differences in multiple domains of behavior, cognition, and psychopathology (Meltzer et al., 2003; Rutter et al., 2003; Roalf et al., 2014). Several of these domains are subserved by distributed neural systems involving both cortical and

Received Aug. 25, 2015; revised Jan. 5, 2016; accepted Jan. 11, 2016.

Author contributions: P.K.R., J.N.G., J.B., and A.R. designed research; P.K.R., L.C., J.B., J.P.L., M.M.C., and A.R. performed research; J.P.L. and M.M.C. contributed unpublished reagents/analytic tools; P.K.R. and A.R. analyzed data; P.K.R., L.C., and A.R. wrote the paper.

This work was supported by the National Institutes of Health (NIH) Intramural Research Program and the NIH Medical Research Scholars Program, a public-private partnership supported jointly by the NIH and generous contributions to the Foundation for the NIH from the Doris Duke Charitable Foundation, The American Association for Dental Research, The Howard Hughes Medical Institute, and the Colgate-Palmolive Company, as well as other private donors. We thank the participants and families who took part in this study. The views expressed in this article do not necessarily represent the views of the NIMH, NIH, HHS, or the United States Government.

The authors declare no competing financial interests.

Correspondence may be addressed to Kirk Reardon, Developmental Neurogenomics Unit, Child Psychiatry Branch, 10 Center Drive, Building 10, Room 3D42, Bethesda, MD 20892. E-mail: kirk.reardon@nih.gov.

DOI:10.1523/JNEUROSCI.3195-15.2016

 0270-6474/16/362438-11$15.00/0

**Table 1. Participant characteristics**

| | Core sample | | | | | | | |
|---|---|---|---|---|---|---|---|---|
| Characteristic | XX | XY | XXX | XXY | XYY | XXYY | XXXXY | Sample for allometric analyses |
| Sample size | 87 | 97 | 23 | 38 | 19 | 15 | 5 | 70 (33 female/37 male) |
| Age, years | | | | | | | | |
| Mean | 12.75 | 12.94 | 12.98 | 14.15 | 13.56 | 14.98 | 12.85 | 13.04 |
| SD | 4.40 | 4.10 | 6.00 | 4.8 | 5.1 | 5.7 | 4.8 | 0.6 |
| Range | 5.16–25.13 | 5.57–25.50 | 5.02–24.78 | 5.89–25.97 | 6.45–23.05 | 5.07–22.96 | 7.66–17.17 | 12.02–13.99 |
| Mean IQ | | | | | | | | |
| Full-scale* | 113.50 | 118.00 | 95.04 | 97.05 | 87.19 | 82.93 | 55.67 | 115.7 (12.7) |
| Verbal* | 114.40 | 115.40 | 95.26 | 95.30 | 83.19 | 77.14 | 60.67 | 113.9 (12.5) |
| Performance* | 111.80 | 115.60 | 95.57 | 99.22 | 94.38 | 92.93 | 56.00 | 113.7 (12.5) |
| SES | | | | | | | | |
| Mean* | 53 | 73 | 42 | 56 | 59 | 46 | 69 | 35.5 |
| Tanner stage $^{+}$ | | | | | | | | |
| 1 | 19 | 16 | 5 | 9 | 6 | 5 | 2 | 2 |
| 2 | 10 | 16 | 3 | 6 | 2 | 2 | 1 | 8 |
| 3 | 17 | 28 | 6 | 9 | 6 | 2 | 1 | 25 |
| 4 | 25 | 16 | 5 | 6 | 3 | 5 | 1 | 29 |
| 5 | 13 | 15 | 4 | 7 | 2 | 1 | 0 | 2 |
| Not known | 3 | 6 | 4 | 1 | 0 | 0 | 1 | 4 |

*$p < 0.01$ for omnibus test of significant variation across groups in core sample.

$^{+}p = 0.03$ for $\chi^2$ test for nonrandom distribution of Tanner stage between sexes in allometric sample. Females in allometric sample show an expected pubertal advancement relative to males as reflected by the distribution of Tanner stages by sex.

subcortical structures (Bradshaw and Sheppard, 2000; Grahn et al., 2008; Kim et al., 2013). Although advances in structural neuroimaging have been leveraged to map sex-differences in human cortical anatomy at high spatiotemporal resolution (Raznahan et al., 2010; Escorial et al., 2015; Giedd et al., 2015), most studies of sex-differences in subcortical anatomy have examined bulk volumes rather than fine-mapping anatomical variation within each nucleus (Sowell et al., 2002; Ostby et al., 2009; Brain Development Cooperative Group, 2012; Rijpkema et al., 2012; Lentini et al., 2013; Wierenga et al., 2014). Moreover, very little is known regarding the potential influence of sex-specific biological factors, such as sex-steroids or sex-chromosome dosage on human subcortical anatomy. Here, we use recently developed methods for analysis of subcortical size and shape (Chakravarty et al., 2013) in a rare neuroimaging cohort of humans with a range of sex-chromosome dosages (Raznahan et al., 2016) to: (1) provide a detailed picture of normative sex-differences in subcortical size and shape, and (2) to test whether these sex-differences might reflect X- and/or Y-chromosome dosage effects.

We focus on sex-chromosome dosage (SCD) as a potential mechanistic contributor to phenotypic sex-differences because disparity in X- and Y-chromosome dosage is the foundational biological sex-difference that distinguishes all male and female eutherian mammals (Hughes and Rozen, 2012). Moreover: (1) studies in transgenic mice have established the presence of gonad-independent SCD effects on both cortical and subcortical anatomy (Corre et al., 2014; Raznahan et al., 2014), and (2) neuroimaging studies in human sex-chromosome aneuploidy (SCA) have established that changes in X- and Y-chromosome count can modify the anatomy of cortical regions with known subcortical projections (Bryant et al., 2011, 2012; Hong et al., 2014; Raznahan et al., 2016). To date however, it is not known whether and how SCD influences subcortical morphology in humans. Addressing these questions would both inform our mechanistic understanding of normative sex-differences in subcortical organization, and identify potential subcortical substrates for the cognitive-behavioral alterations that are associated with SCA (Hong and Reiss, 2014).

Our study design integrates several methodological strengths in its assessment of sex and SCD effects on subcortical anatomy. First, we conduct a combined study of the striatum, pallidum, and thalamus using multi-atlas methods that model variations in both the bulk volume and local shape of each structure (Chakravarty et al., 2013; Raznahan et al., 2015). Second, we leverage multiple karyotype groups (XX, XXX, XY, XXY, XYY, XXYY, and XXXXY) to: (2) directly compare sex, X- and Y-chromosome effects, and (2) conduct sensitivity analyses that examine the same chromosome-dosage change across different gonadal contexts (e.g., a supernumerary X-chromosome in both XXX and XXY).

Finally, we embed all our findings within an allometric framework by using an independent sample of 70 typically developing individuals to generate the first normative models of global and local scaling of subcortical anatomy with overall brain size in humans. Because brain regions can vary in their scaling relationships with overall brain size (Toro et al., 2009), and sex and SCD robustly alter overall brain size (Raznahan et al., 2016), allometric norms are required to distinguish whether regionally specific effects of sex and SCD on brain anatomy arise as a consequence of regional differences in scaling, or actually represent focal anatomical deviations from the norm given overall brain size differences. To demonstrate the importance of allometry, we also analyze sex and SCD effects on subcortical anatomy while controlling for brain size using two "classical" methods that both assume linear scaling: normalization of regional volumes by total brain volume, and use of statistical models that include the linear effects of total brain volume as a "nuisance" variable.

## Materials and Methods

*Participants*

The core sample for this study included 284 individuals representing a range of karyotypes: 87 XX, 97, XY, 38 XXY, 23 XXX, 19 XYY, 15 XXYY, and 5 XXXXY. A non-overlapping sample of 70 typically developing individuals (33 female and 37 male) aged 12–14 years was used to construct normative allometric scaling laws for subcortical volume and shape at the mean age of our core sample (Table 1).

Sex-chromosome aneuploidy groups were recruited through advertisements via the NIH website and parent-support groups across North America. To be included in the study, participants must have had an X-/Y-aneuploidy and not ever had a head injury or condition that would result in gross brain abnormalities. All participants with aneuploidy were

non-mosaic. Typically developing participants were all singletons recruited from the United States of America and enrolled in ongoing longitudinal study of typical brain development (ClinicalTrials.gov identifier: NCT00001246, NIH Annual Report Number: ZIA MH002794-13) (Giedd et al., 2015). Inclusionary criteria for healthy participants included never having required special education services, taken psychiatric medications, received mental health treatment, or having had any medical condition impacting the nervous system.

### *Neuroimaging*

All structural magnetic resonance imaging (sMRI) brain scans were T1-weighted images with contiguous 1.5 mm axial slices and obtained on the same 1.5-T General Electric Signa scanner using a 3D spoiled-gradient recalled-echo sequence with the following image acquisition parameters: echo time, 5 ms; repetition time, 24 ms; flip angle, 45°; acquisition matrix, 256 × 192; number of excitations, 1; and field-of-view, 24 cm.

Fully automated subcortical segmentation and surface extraction was achieved using the previously described MAGeT Brain algorithm (Chakravarty et al., 2013). To summarize the technique, 3D reconstruction of serial histologic data for the striatum, pallidum, and thalamus were warped to an MRI-based template (Chakravarty et al., 2006). The atlases were then customized to a subset of the dataset (30 randomly selected subjects) using a nonlinear transformation estimated in a region-of-interest defined around the subcortical structures. This set of subjects then acts as a set of templates to which all other scans are warped. This procedure provides thirty candidate subcortical segmentations for each scan. The final segmentation is decided upon using a voxelwise majority vote; that is, the label occurring most frequently at a specific location is retained. These methods are reliable in comparisons against "gold standard" manual definitions (Dice kappa = 0.86). A quality control image file is provided for each scan, allowing detailed visual inspection to rule out the presence of segmentation errors. All scans included in these analyses passed quality control of raw scans and MAGeT Brain segmentations for motion artifact and other confounders by two independent raters who were blinded to subject karyotype.

To determine shape, surface-based representation of subcortical structures defined on the input atlas were first estimated using the marching cubes algorithm and then morphologically smoothed using the AMIRA software package (Visage Imaging). Next, the nonlinear portions of the 30 transformations mapping each subject to the 30 input templates were concatenated and averaged across the template library to limit the effects of noise and error and to increase precision and accuracy. These surface based representations were warped to fit each template, and as in the case of the segmentation, each of these surfaces was warped to match each subject. This procedure yields 30 possible surface representations per subject that are then merged by creating a new surface representation of the striatum/thalamus or pallidum but estimating the median coordinate representation at each location. At this point, one-third of the surface of each triangle is assigned to each vertex within the triangle. The surface area value stored at each vertex is the sum of all such assignments from all connected triangles. Finally, surface-area values were blurred with a surface based diffusion-smoothing kernel (5 and 3 mm for the striatum/thalamus and pallidum, respectively). The measures of interest generated by this processing stream for each scan were total volume estimates for left and right striatum, pallidum, and thalamus (summed to provide a single estimate of total bilateral volume for each structure) and surface area at a total of 21,156 vertices across all structures (striatum, 6450 left/ 6178 right; pallidum, 1266 left/1138 right; thalamus, 3016 left/ 3108 right). To derive measures of total brain tissue volume (TBV; total gray matter volume + total white matter volume) for allometric analyses, we submitted all scans to the previously described CIVET pipeline (Ad-Dab'bagh et al., 2006) for automated morphometric analysis.

### *Statistical analyses*

*Participant characteristics.* Continuous (e.g., age at scan) and categorical (e.g., Tanner stage) characteristics were compared across karyotype groups in our core sample and across sex in our non-overlapping sample of typically developing participants using omnibus ANOVA *F* tests and $\chi^2$ tests, respectively.

*Sex and sex-chromosome dosage effects on subcortical volume.* We calculated mean striatal volume (SV), thalamic volume (TV), and pallidal volume (PV) for each karyotype group within our core sample. For each structure, karyotype effects on volume were first quantified using omnibus *F* tests. For structures showing a significant omnibus effect of group, follow-up *post hoc* pairwise *t* tests were used to clarify the pattern of volumetric group-differences. We explicitly tested for, and ruled out, significant interactions between: (1) X-aneuploidy status (no aneuploidy vs supernumerary X) and gonadal sex (male vs female), and (2) X-and Y-aneuploidy status, using linear models in relevant subsets of our sample [(XY, XXY, XX, XXX), and (XY, XXY, XYY, XXYY) respectively]. To facilitate comparison across structures, mean structure volumes (±95% CI) were plotted by karyotype group as effect-size deviations relative to volume distributions in typically developing males (see Fig. 2; XY and XXX) or females (see Fig. 2; XX, XXY, XYY, and XXYY).

*Allometry of subcortical volumes.* We used an independent sample of 70 typically developing individuals to calculate normative allometric relationships between TBV and the volume of each subcortical structure. For each subcortical structure, normative scaling laws were estimated using the following equation (using TV as an example):

$$\log10\ (\text{Bilateral Thalamic Volume}) \sim \beta_0(\text{Intercept}) + \beta1(\log10(\text{TBV})). \quad (1)$$

Here, $\beta_1$ provides the estimated scaling coefficient linking variation in TV to variation in TBV. A $\beta_1$ value of 1 indicates linear scaling (i.e., proportional TV remains unchanged with variations in brain size), with $\beta_1$ values $<1$ indicating hypoallometric scaling (i.e., proportional thalamic volume becomes smaller with increasing brain size), and $\beta_1$ values $>1$ indicating hyperallometric scaling (i.e., proportional TV becomes larger with increasing brain size). For all three structures examined, Equation 1 was run after first establishing the absence of significant interactions between sex and log10(TBV) in predicting structure volume. For the pallidum, sex was retained as a main effect given evidence for a TBV-invariant increase in mean PV among males relative to females. Next, having estimated these normative scaling laws for each subcortical structure, we tested whether the subcortical volumes observed in each karyotype group within our core sample: (1) fell within the range predicted by the observed change in TBV given normative brain allometry, or (2) represented a statistically significant disruption of the normative relationship between structure volume and TBV (see Fig. 2). A significant deviation from allometric expectations was operationalized as a lack of overlap between the 95% confidence intervals for the observed and predicted mean structure volume in each karyotype group. As a comparison for these allometric analyses, we also modeled sex and sex-chromosome effects on subcortical volume using the two traditional (non-allometric) approaches to accounting for brain size when studying regional brain volumes: expressing regional volumes as a ratio of TBV, and including the linear effect of TBV as a covariate in regression analyses.

*Sex and sex-chromosome dosage effects on subcortical shape.* We estimated normative sex-differences in subcortical shape between the XX and XY participants in our core sample, by modeling local area at all subcortical vertices using the following equation:

$$\text{Vertex Area} \sim \beta_0(\text{Intercept}) + \beta_1(\text{Age} - \text{Mean\_Age}) + \beta_2(\text{Sex}). \quad (2)$$

Regions showing significant sex-differences in subcortical shape were visualized by projecting vertex-wise $\beta_2$ coefficients onto exemplar subcortical surfaces after applying a false discovery rate (FDR) correction for multiple comparisons (Genovese et al., 2002) with $q$ (the expected proportion of falsely rejected null hypotheses) set at 0.05. Equation (2) was applied at all vertices after first testing for and ruling out statistically significant interactions between age and sex in predicting vertex area.

To provide an independent yet complementary view of sex-differences in subcortical shape that accounts for sex-differences in the overall size of each structure, we ran the following vertex-wise analysis within our non-overlapping allometric sample of typically developing controls (using the striatum as an example):

| CHARACTERISTIC | KARYOTYPE | | | | | | | Omnibus test for group difference | |
|---|---|---|---|---|---|---|---|---|---|
| | XX | XY | XXX | XXY | XYY | XXYY | XXXXY | *F* statistic | *P*-value |
| TBV ($cm^3$) | | | | | | | | | |
| Mean | 1254.31 | 1400.77 | 1165.73 | 1292.03 | 1407.84 | 1260.90 | 1131.06 | 26.28 | <2.2*10-16 |
| SEM | 11.9 | 16.4 | 26.0 | 21.6 | 28.1 | 31.0 | 51.0 | | |
| SV ($cm^3$) | | | | | | | | | |
| Mean | 17.31 | 18.47 | 15.69 | 17.01 | 18.30 | 16.29 | 14.84 | 13.70 | 1.257*10-13 |
| SEM | 0.2 | 0.3 | 0.4 | 0.3 | 0.4 | 0.5 | 0.8 | | |
| TV ($cm^3$) | | | | | | | | | |
| Mean | 11.21 | 12.08 | 10.47 | 11.28 | 11.72 | 10.88 | 9.67 | 17.60 | <2.2*10-16 |
| SEM | 0.1 | 0.1 | 0.2 | 0.2 | 0.2 | 0.3 | 0.4 | | |
| PV ($cm^3$) | | | | | | | | | |
| Mean | 2.42 | 2.62 | 2.12 | 2.33 | 2.43 | 2.11 | 1.70 | 32.32 | <2.2*10-16 |
| SEM | 0.0 | 0.0 | 0.5 | 0.0 | 0.1 | 0.1 | 0.1 | | |

***P< 0.001, **P< 0.01, *P< 0.05


**Figure 1.** Indices of global and subcortical brain anatomy in each karyotype with *post hoc* pairwise comparisons for each karyotype pair. Group mean values, estimates of error, and omnibus test statistics for each anatomical metric were determined using $\beta_1$ coefficients from the following model: anatomy ~ intercept + $\beta_1$(group). Color bar encodes level of statistical significance for the cross-tabulated *post hoc* pairwise comparisons.

$$\log10(\text{Vertex Area}) \sim \beta_0(\text{Intercept}) + \beta_1 \times (\log10\ (\text{Total Bilateral Striatal Surface Area}) + \beta_2(\text{Sex}). \quad (3)$$

The $\beta_2$ coefficient was visualized after correction for multiple comparisons, and identified regional sex-differences in subcortical shape that exist above and beyond sex-differences on overall subcortical size.

Next, to map the areal sensitivity of subcortical shape to sex-chromosome dosage effects we defined groups of vertices that shared a common pattern of areal response to the variations in X- and Y-chromosome dosage represented in our sample. To achieve this, we first re-expressed mean vertex-wise surface area (SA) measures in each SCA group as effect-size deviations from SA distributions at homologous vertices in the appropriate gonadally matched control group (i.e., XXX mean against the XX distribution/XXY, XYY, XXYY, and XXXXY means against the XY distribution). These steps resulted in a matrix of 21156 rows (all subcortical vertices) and 5 columns (effect-size for SA in each SCA group vs its gonadal control). This matrix was then submitted to a *k*-means partitioning algorithm ["kmeans" function in the R language and environment for statistical computing (Cahill, 2006); with iter.max and nstart set at 100], and an optimal four-cluster solution was indicated by visual inspection of a scree-plot charting reduction in the mean within-partition sums of squares against increasing partition number. Vertex-wise cluster designations according to this four-class solution were visualized on exemplar subcortical surfaces using color codes. A $\chi^2$ analysis was used to quantitatively describe the nonrandom distribution of clusters across subcortical nuclei.

The above approach was adopted to provide an integrated picture of SCA effects on subcortical anatomy. Supplementary vertex-wise group contrasts between each SCA and their gonadal control (using an identical approach to that detailed in Eq. 2 above) identified statistically significant effects of each separate SCA on regional cortical anatomy that corroborated the integrated summary provided by *k*-means analysis.

*Allometry of subcortical shape.* The same independent sample of 70 typically developing controls used to model normative allometry of subcortical volume was used to estimate structure-specific allometric scaling laws for all four subcortical partitions defined by *k*-means analysis above. These normative scaling laws were estimated in a stepwise manner for each unique cluster-structure pairing. We first tested for significant sex-differences in normative allometry using the following equation:

$$\log10(\text{K Cluster Area}) \sim \text{Intercept} + \beta_1 \times (\log10(\text{Total Bilateral Surface Area})) + \beta_2(\text{Sex}) + \beta_3(\text{Sex} * \log10\ (\text{Total Bilateral Surface Area})). \quad (4)$$

For cluster–structure pairings where the $\beta_3$ terms failed to reach statistical significance, we stepped-down to the following equations, depending on the presence/absence (Eqs. 5 and 6, respectively) of a statistically significant main effect of sex:

$$\log10(\text{K Cluster Area}) \sim \text{Intercept} + \beta_1 \times (\log10(\text{Total Bilateral Surface Area})) + \beta_2(\text{Sex}), \quad (5)$$

$$\log10(\text{K Cluster Area}) \sim \text{Intercept} + \beta_1 \times (\log10(\text{Total Bilateral Surface Area})). \quad (6)$$

Finally, in a manner analogous to that used for subcortical volumes, we assessed whether observed cluster areas in each SCA group were congruent with what would be expected given the observed change in the overall size (total bilateral surface area) of each subcortical structure, and the cluster-specific allometric relationships defined above.

*Tests for effects of demographic, pubertal and cognitive factors.* For all analyses of sex-chromosome dosage effects on subcortical anatomy within our core sample, we ran additional models that confirmed robustness of our findings to inclusion of socioeconomic status (SES) as a covariate. We did not covary for IQ in analyses of sex-chromosome aneuploidy effects because: (1) IQ reductions are central to the sex-chromosome aneuploidy phenotype, and (2) inclusion of IQ as a nuisance variable in regression analyses assumes the presence of a linear relationship between IQ and brain anatomy that is invariant across karyotype groups.

Within our non-overlapping normative sample, we ran additional models that confirmed the robustness of all reported sex-differences in subcortical allometry to inclusion of Tanner stage, IQ, and SES as covariates.

## Results

### Sex and sex-chromosome dosage effects on subcortical volumes

Mean SV, PV and TV each differed significantly across karyotype groups, as did TBV (Fig. 1). Relative to karyotypically normal females, karyotypically normal males showed increased TBV in addition to increased SV, PV, and TV. The effects-size for male–female differences in TBV was greater than the effect sizes for male–female differences in all three subcortical volumes (Fig. 2). Sex-chromosome aneuploidies in both males and females were associated with large-effect size reductions in total brain, SV, PV, and TV (Figs. 2), with the sole exception of the XYY karyotype which only resulted in a statistically significant reduction of TV and PV relative to XY males. Across all SCAs, effect sizes for absolute PV volume loss outstripped those seen in the striatum and thalamus. Supplementary analyses established that the effects of X-chromosome aneuploidy

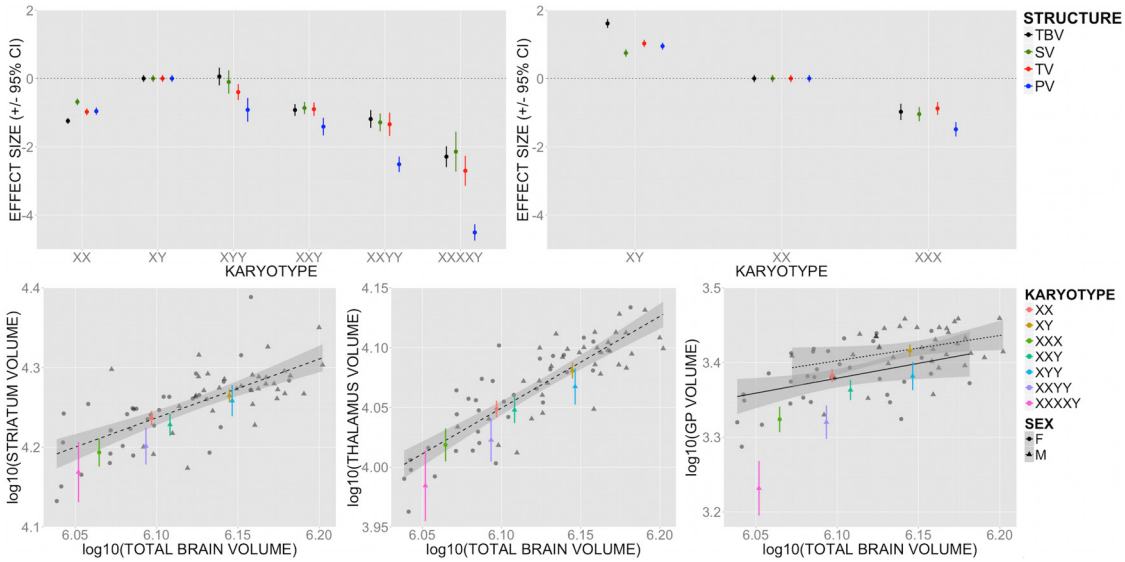


**Figure 2.** Total brain, thalamic, pallidal, and striatal volumes across sex-chromosome karyotype groups. Top, TBV, SV, TV, and PV in karyotype groups expressed as mean (±95% CI) effect-size deviations according to observed distribution in males and females. The contrast between karyotypically normal males and females is included in both panels to allow easy comparison of sex and sex-chromosome effects within each gonadal context. Bottom, Subcortical volume findings in our core sample in the context of normal brain allometry. Gray points and fit-lines (see Table 2 for associated coefficients) show the log–log relationship between TBV and each subcortical volume in an independent sample of typically developing males an females. Superimposed points show observed distributions of SV, TV, and PV at mean TBV for each karyotype groups within our core sample (groups color-coded).

**Table 2. Allometry of subcortical volume in health**

| | Normative scaling coefficients | |
|---|---|---|
| Structure | Allometric coefficient (±95% CI) | Male intercept offset (±95% CI) |
| Striatum | 0.74 (±0.188)** | — |
| Pallidum | 0.37 (±0.2231)*** | 0.022 (±0.019)* |
| Thalamus | 0.77 (±0.119)*** | — |

Normative allometric coefficients, male-related intercept offsets and associated $p$ values for the scaling of each subcortical nucleus volume with TBV as significantly different from 1.

***$p < 0.001$, **$p < 0.01$, *$p < 0.05$.

were not modified by gonadal sex ($p$ values for global and regional anatomy were all >0.6 for the interaction between X-chromosome supernumeracy and sex using the XX, XXX, XY, XXY participant subset), or Y-chromosome aneuploidy ($p$ values for global and regional anatomy contrasts were all >0.2 for the interaction between X- and Y-chromosome supernumeracy using the XY, XXY, XYY, XXYY subset).

## Allometry of subcortical volumes

Our models of normative allometry revealed that SV, PV, and TV all show hypoallometric scaling with TBV in health (Table 2) meaning that across individuals, larger brains have proportionally smaller subcortical volumes than smaller brains. The magnitude of this hypoallometric scaling was significantly more marked for PV volume versus TV and SV. None of the three structures studied showed sexually dimorphic scaling with TBV, although males showed a statistically significant "offset" (increase) in PV volume relative to females, which was consistent across a range of brain volumes.

Comparison of observed subcortical volumes in SCA relative to the predictions of normative brain allometry (Fig. 2) indicated that: (1) the extent of PV volume reduction in all SCAs significantly outstripped what would be predicted from changes in brain size alone, and (2) SV and TV reductions showed a trend toward being disproportionately large in XYY (thalamus), XXYY (thalamus and striatum), and XXXXY (thalamus and striatum) groups relative to observed changes in TBV.

**Table 3. Comparing different methods of controlling for brain size in analysis of subcortical volume**

| | vs XX | | vs XY | | | |
|---|---|---|---|---|---|---|
| | XY | XXX | XXY | XYY | XXYY | XXXXY |
| Striatum | | | | | | |
| Normalization | ↓ | — | — | — | — | — |
| Covarying | — | ↓ | — | — | ↓ | — |
| Allometry | — | — | — | — | — | — |
| Thalamus | | | | | | |
| Normalization | ↓ | — | — | ↓ | — | — |
| Covarying | — | — | — | ↓ | ↓ | ↓ |
| Allometry | — | — | — | — | — | — |
| Pallidum | | | | | | |
| Normalization | ↓ | ↓ | ↓ | ↓ | ↓ | ↓ |
| Covarying | ↑ | ↓ | ↓ | ↓ | ↓ | ↓ |
| Allometry | ↑ | ↓ | ↓ | ↓ | ↓ | ↓ |

Subcortical volumes were compared between each SCA group and their "gonadal control" using three different methods to control for total brain size variation: normalizing by total brain volume, covarying by total brain volume, and using our new allometric framework.

Arrows indicate presence and direction of statistically significant group difference in the volume of each structure at $p < 0.05$.

In keeping with our observation that the volume of all three subcortical structures studied scaled in a nonlinear fashion with TBV, we found that classical methods of "controlling for" TBV differences, which both assume linear scaling between regional volumes and TBV, conflated the effects of nonlinear scaling with the effects of sex and SCA on subcortical anatomy (Table 3).

## Sex and sex-chromosome dosage effects on subcortical shape

Vertex-wise analyses of sex-differences in local subcortical surface area indicated that the subcortical volumetric increases observed in karyotypically normal males relative to females were not associated with even areal expansion throughout each subcortical structure studied (Fig. 3*A*). A set of bilaterally symmetric subcortical regions failed to show significant areal expansion in males relative to females, including rostromedial facets of the caudate body, the rostral putamen, rostral pallidum, and both paraven-

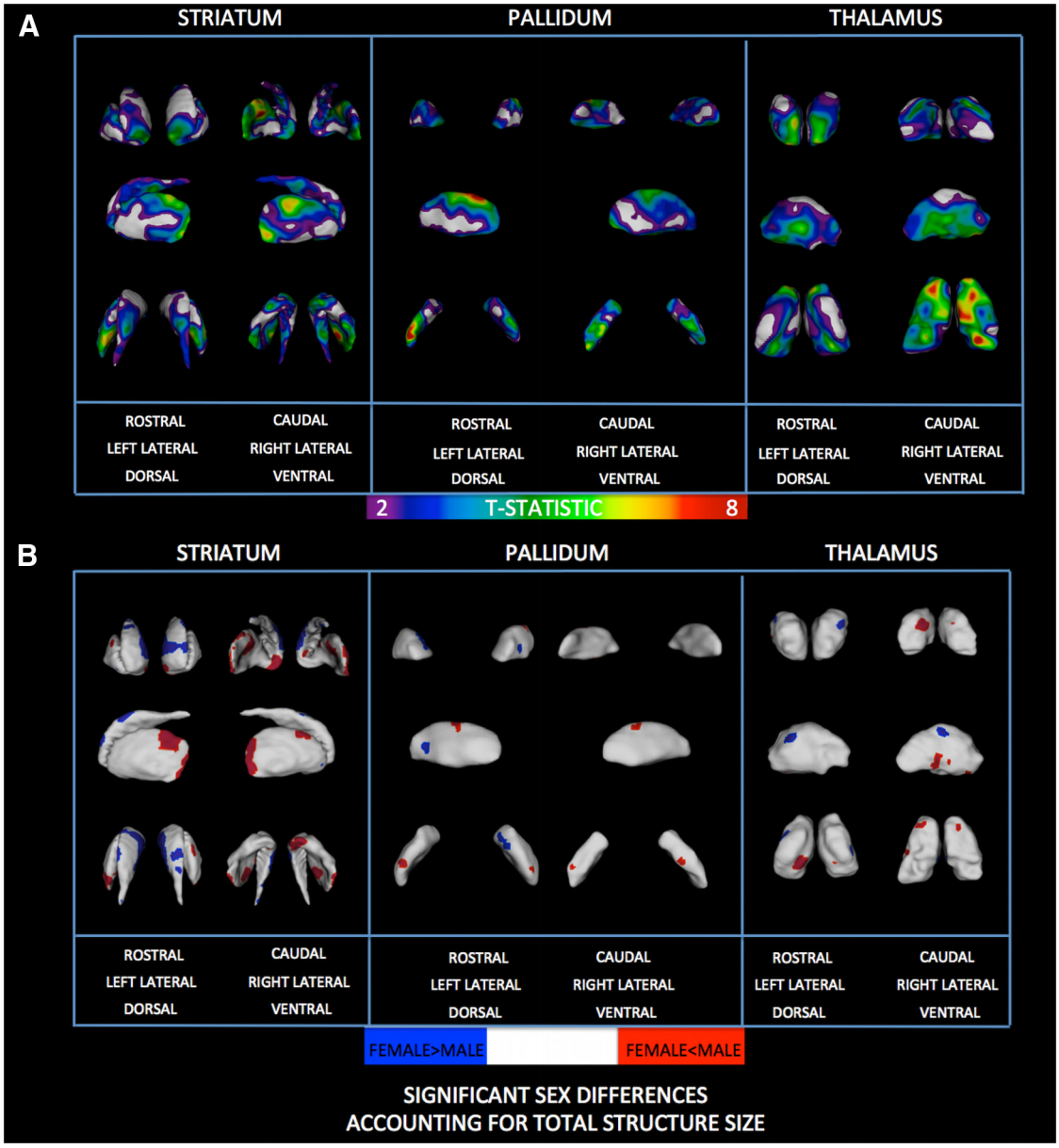


**Figure 3.** Normative sex-differences in striatal, pallidal, and thalamic shape. ***A***, Colored regions denote significant areal expansion in males relative to females after FDR correction for multiple comparisons. Warmer colors denote more pronounced areal expansion in males. Gray regions denote regions of statistical areal equivalence between males and females. There were no regions of significant areal contraction in males relative to females. ***B***, Normative sex-differences accounting for allometry of global effects. Colors denote regions with significant sex-differences in surface area in each structure after accounting for the nonlinear effects of overall structure size (after FDR correction for multiple comparisons; red: M>F; blue: F>M).

tricular and dorsal facets of the thalamus. Conversely, regions of statistically significant subcortical areal expansion in males relative to females were not homogeneous in the observed magnitude of areal sex-differences: notable "hotspots" of areal expansion in males versus females included the ventral striatum and dorsocaudal putamen, dorsal pallidum, and ventral thalamus. Reanalyzing sex-differences in subcortical shape while accounting for sex-differences in subcortical size within our non-overlapping sample of typically developing controls (Fig. 3*B*) identified: (1) regions of relative areal expansion in males that overlapped with several hotspots where absolute subcortical area was most dramatically increased in males versus females within our core sample, and (2) regions of relative areal expansion in females that overlapped with areas where absolute surface area did not differ between males and females in our core sample despite significant sex-differences in overall subcortical size.

The *k*-means partitioning algorithm used to map sex-chromosome effects on subcortical shape identified four spatially distributed yet bilaterally symmetric subcortical domains with different anatomical responses to changes in X- and Y-chromosome dosage (Fig. 4*A*,*B*). The "blue cluster," spanning the caudate tail and dorsal thalamus, exhibited significant areal expansion in SCA groups relative to their gonadally matched controls. In contrast, the "cyan cluster," spanning the caudate body, nucleus accumbens, and ventromedial thalamus, showed a smaller and less consistent areal response to changes in X- and Y-chromosome dosage across groups. All remaining subcortical regions fell within yellow and red clusters. Both these clusters showed robust areal contraction in all sex-chromosome aneuploidy groups relative to gonadal controls, but these reductions were most pronounced within the red cluster, which encompassed rostroventral regions of the striatum, neighboring facets

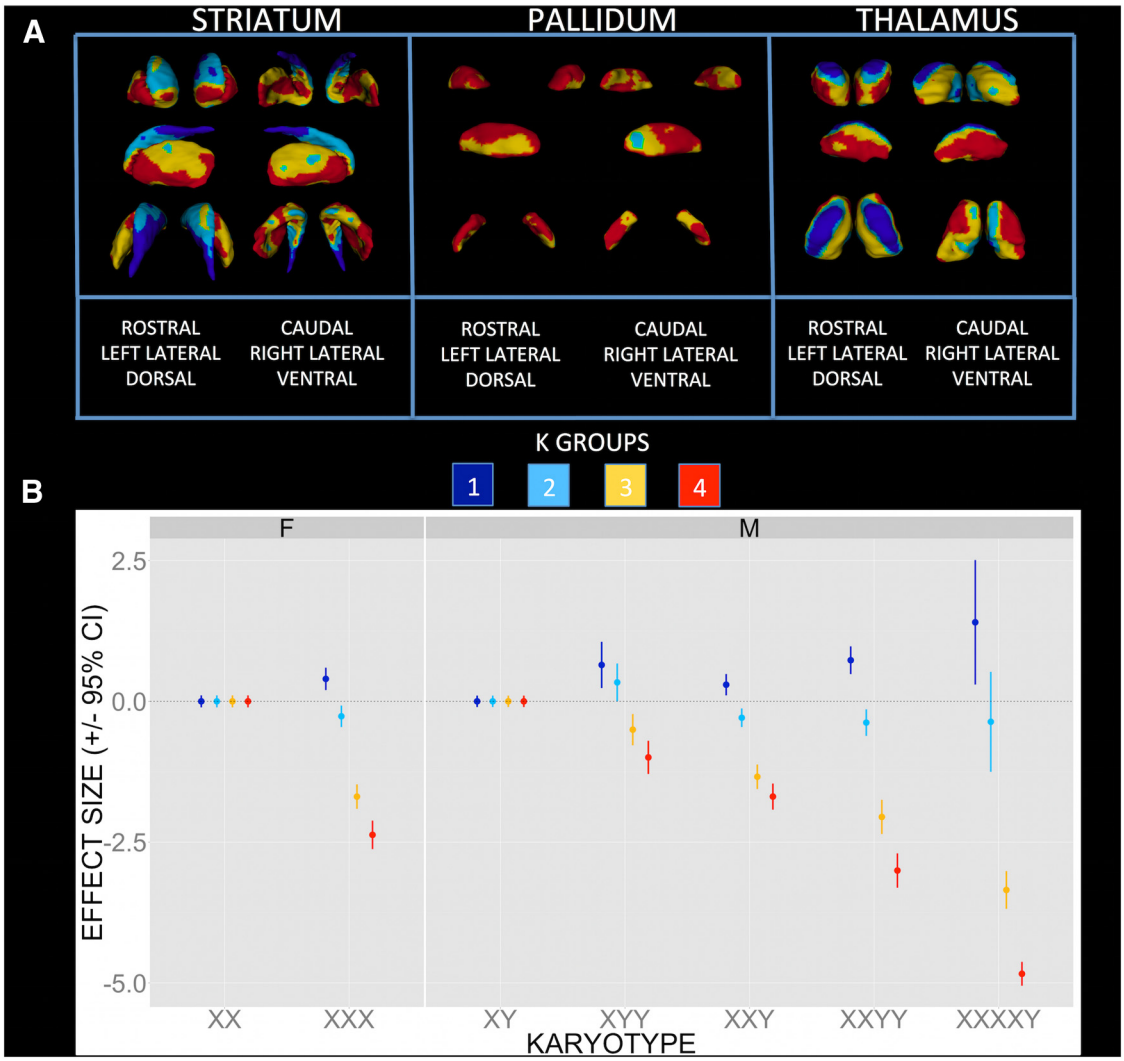


**Figure 4.** Sex-chromosome dosage effects on striatal, pallidal and thalamic shape. ***A***, Vertex-wise maps vertex color distinguishes four spatially distributed subcortical domains with differing patterns of shape-change in response to sex-chromosome aneuploidy. Blue domains are regions that show areal expansion in all SCA groups relative to their respective gonadal control groups. The cyan domain shows smaller and less consistent areal changes with SCA. Remaining subcortical facets fall into a yellow domain of intermediate areal contraction with SCA or a red domain of more marked areal contraction with SCA. ***B***, The mean area of each color-coded domain in each SCA group; expressed as a SD relative to distribution of domain area in that SCAs respective "gonadal control" group.

**Table 4. Standardized residuals for the difference between observed and expected vertex counts in each unique structure–cluster pairing**

| | Cluster | | | |
|---|---|---|---|---|
| Structure | Blue | Cyan | Yellow | Red |
| Striatum | 8.34 | 15.01 | −8.14 | −9.39 |
| Pallidum | −17.54 | −22.83 | −0.57 | 29.62 |
| Thalamus | 3.25 | −0.79 | 9.2 | −10.57 |

The striatum is enriched for blue and cyan clusters, the thalamus for blue and yellow, and the pallidum for red.

of the pallidum and the lateral thalamus. These four clusters were not evenly distributed across all three subcortical structures: the blue cluster was relatively enriched in the striatum and completely absent from the pallidum; the cyan cluster was enriched in the striatum and thalamus but underrepresented in the pallidum; whereas the yellow and red cluster were relatively enriched within the thalamus and pallidum (Table 4).

### Allometry of subcortical shape

Given the significant effects of sex and SCA on the overall size of each subcortical structure (Fig. 1), the regionally specific effects of these factors on subcortical shape (Fig. 4) could potentially be wholly reflective of regional differences in the normative allometry of each subcortical nucleus. To examine this possibility, we constructed normative scaling laws to describe how the relative size of each *k*-means cluster varied with the total size of each subcortical structure in health (Fig. 5). Comparison of the observed effects of SCA on regional subcortical area with regional areal changes predicted from normative allometry revealed that only a subset of regional SCA effects on subcortical shape reflected unexpected deviations from what would be predicted by normative allometry alone: XXX, XXY, XXYY, and XXXXY effects on the area of blue and red domains within the striatum and thalamus.

Our models of normative allometry within each *k*-means cluster also pointed toward regionally heterogeneous scaling of subcortical shape in health (Table 5). For example, blue and cyan clusters within the striatum and thalamus all showed disproportionate areal expansion with increasing structure size. In contrast, red clusters in the striatum and thalamus became proportionally smaller with increasing structure size. We also noted that norma-

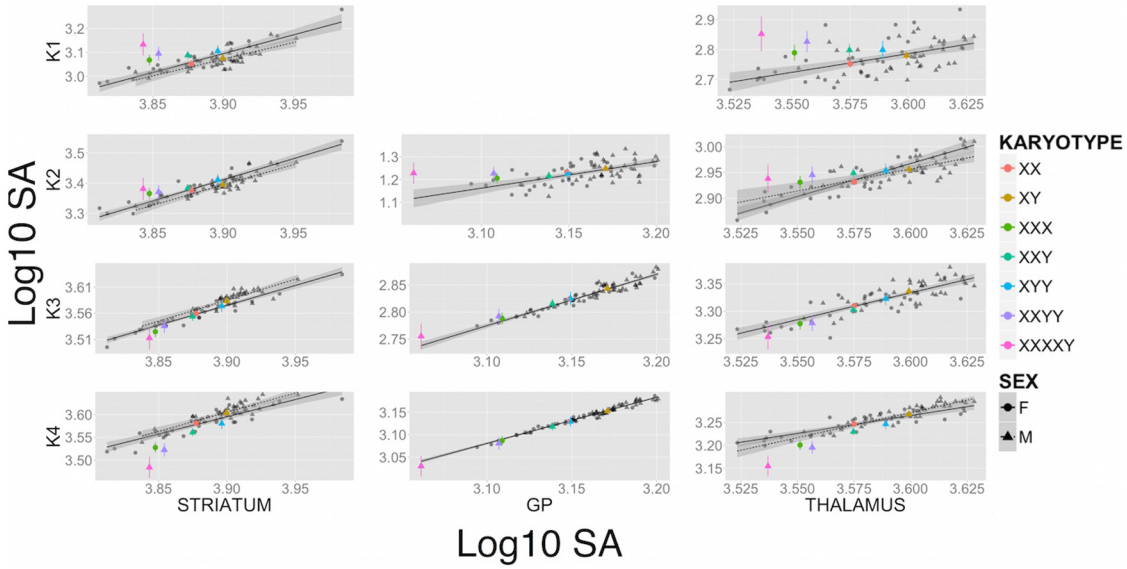


**Figure 5.** Regional allometry of subcortical shape by *k*-mean clusters. These scatterplots display observed distributions of regional *k*-mean group SA relative to total SA of its respective nucleus for all karyotypes within our core sample (color-coded), relative to scaling relationships observed in an independent sample of typically developing controls (sex-shape coded) with annotations for sex-effect in intercept and slope.

**Table 5. Scaling of regional subcortical area with overall structure size in health**

| | Structure | | |
|---|---|---|---|
| Cluster | Allometric coefficient (±95% CI) | Male intercept offset (±95% CI) | Male slope (±95% CI) |
| Striatum | | | |
| Blue | 1.53 (±0.224)*** | −0.02 (±0.014)** | — |
| Cyan | 1.38 (±0.139)*** | −0.02 (±0.008)*** | — |
| Yellow | 0.77 (±0.071)*** | 0.01 (±0.004)*** | — |
| Red | 0.79 (±0.107)*** | 0.01 (±0.007)** | — |
| GP | | | |
| Blue | — | — | — |
| Cyan | 1.17 (±0.382) | — | — |
| Yellow | 0.95 (±0.072) | — | — |
| Red | 1.03 (±0.040) | — | — |
| Thalamus | | | |
| Blue | 1.24 (±0.456) | — | — |
| Cyan | 1.27 (±0.224)* | — | 0.85 (±0.370)* |
| Yellow | 0.98 (±0.153) | — | — |
| Red | 0.78 (±0.142)** | — | 1.09 (±0.233)* |

Allometric coefficients for each unique structure–cluster pairing show how regional surface areas change with the overall size of each subcortical structure. Additional coefficients are provided for clusters that show a statistically significant fixed male intercept offset (±95% CI) or allometrically varying male slope (±95% CI) sex-difference in size.

*$p < 0.05$, **$p < 0.01$, ***$p < 0.001$.

tive scaling relationships within cyan and red clusters of the thalamus were sexually dimorphic such that the observed deviations from isometric scaling within these regions were less pronounced in males than females. Finally, our sample of typically developing males and females showed baseline differences in the proportional size of each cluster within the striatum: blue and cyan clusters were relatively smaller in males than females across all striatal sizes, whereas yellow and red clusters were proportionally larger in males.

## Discussion

### Sex and sex-chromosome dosage effects on subcortical volume

Our findings replicate previous reports that typically developing males show greater mean TBV, SV, PV, and TV than females (Ostby et al., 2009; Brain Development Cooperative Group, 2012), and further establish that the effect-size magnitude of these volume differences is greatest for TBV, intermediate for TV and PV, and least for SV.

Supernumerary sex-chromosomes were associated with subcortical volume reductions. This observation contrasts with the divergent supernumerary X- and Y-chromosome effects on cortical volume (Raznahan et al., 2016), and suggests that normative sex-differences in subcortical volumes are unlikely due to differential sex-chromosome complement. Furthermore, the profile of TBV, SV, PV, and TV change seen with X- or Y-chromosome supernumeracy does not recapitulate the profile of volume differences seen across these structures between typically developing males and females.

### Allometry of subcortical volumes

Our study demonstrates how neglecting normative brain allometry distorts conclusions regarding sex and sex-chromosome effects on subcortical volumes. Our allometric analysis of sex-differences in subcortical volumes concludes that: (1) the striatum and thalamus are proportionally smaller in males due to sex-differences in TBV alone, but (2) PV is proportionally larger in males regardless of TBV. In contrast, analysis of our data using two classical "corrections" for TBV effects, which both fail to account for nonlinear relationships between subcortical volumes and TBV, concludes that male sex imparts smaller SV, TV, and PV (normalization by TBV), or smaller SV and TV, alongside larger PV (covarying for TBV). Our analyses using these classical corrections recapitulate previous findings of normative sex-differences in subcortical volumes using normalization by or covariation for TBV (Ahsan et al., 2007; Rijpkema et al., 2012).

Our allometrically informed analysis of SCA effects on subcortical volumes highlights the special vulnerability of PV to supernumerary sex-chromosome dosage (Table 3). Speculatively, this vulnerability could reflect the sensitivity of pallidal neurons to oxidative stress (Johnston, 2001), given that aneuploidy states

are known to modify the expression of genes related to oxidative stress (Sheltzer et al., 2012).

Our allometric analyses also establish for the first time that SV, PV, and TV all scale sublinearly with TBV in humans. This feature of brain scaling in health aligns with established sublinear scaling of the putamen and diencephalon with increasing TBV across diverse species (Finlay and Darlington, 1995). Thus, both within humans and across species, the disproportionate expansion of cortical volume with greater TBV (Finlay and Darlington, 1995; Raznahan et al., 2016) does not require commensurate increases in subcortical volume.

**Sex and sex-chromosome effects on local subcortical anatomy**

Our vertex-wise analyses show that greater SV, TV, and PV in males relative to females is not associated with evenly distributed sex-differences in subcortical surface area. Specifically, subcortical regions of areal sex-equivalence include the caudate head, ventral putamen, neighboring rostral facets of the lateral and medial pallidum, and dorsomedial regions of the thalamus; whereas, regions of prominent areal expansion in males include the ventral striatum, the mid-tail of the caudate, dorsal putamen and pallidum, as well as rostral and ventral facets of the thalamus. Notably, striato-thalamic regions that are statistically indistinguishable between males and females share functional associations with orbitofrontal and lateral prefrontal cortices; whereas, regions of pronounced areal increase in males versus females show strongest functional connectivity with cingulo-opercular and motor cortices (Choi et al., 2012; Greene et al., 2014).

Our study also demonstrates regionally specific supernumerary sex-chromosome dosage effects on subcortical shape. Using a data-driven method, we distinguish four subcortical domains with differing responses to SCA. Without any a priori constraints, the subcortical domains detected by our method: (1) show striking bilateral symmetry, (2) integrate neighboring facets across different structures (e.g., blue domains in caudate tail and dorsal thalamus; Fig. 3), and (3) define a ventrodorsal gradient of sex-chromosome dose effects on striatal and thalamic surface area that recapitulates a major topographic axis of corticostriato-thalamic connectivity (Voorn et al., 2004; Draganski et al., 2008; Choi et al., 2012).

X- and Y-chromosome dose have similar areal effects to each other within blue, yellow, and red subcortical domains, with greater sex-chromosome dose imparting greater anatomical changes. Thus, in keeping with our previous study of cortical anatomy in SCA (Raznahan et al., 2016), the present study identifies convergent X- and Y-chromosome effects on regional subcortical anatomy. Our data hint at a possible alignment between the spatial patterning of SCA effects on cortical and subcortical anatomy. For example, available maps of functional connectivity between the human caudate and cortex (Choi et al., 2012; Greene et al., 2014) pair subcortical and cortical regions which we find have shared anatomical vulnerability (anterior cingulate, caudate head) or resilience (dorsolateral prefrontal cortex, caudate body) to SCA effects. Coherence between the spatial patterning of SCA effects within and between cortical and subcortical structures provides a candidate systems-level framework for investigating the functional anatomy of documented changes in motor development, language, attention, and mood that can accompany SCA (Tartaglia et al., 2008; Lee et al., 2012; Blumenthal et al., 2013; Hong and Reiss, 2014).

**Allometry of subcortical shape**

Our study demonstrates that regional subcortical allometry in health provides a critical context for the study of SCA effects on subcortical shape; e.g., only through allometric analysis does it emerge that X- and Y-chromosome supernumeracy preserves pallidal shape (despite dramatically reducing PV), while distorting striatal and thalamic shape. Intriguingly, these distortions counter the shape changes predicted by SCA effects on SV and TV assuming normative brain allometry. Hyperallometric blue domains, which should show disproportionate areal contraction as SV and TV reduce with mounting sex-chromosome dose, actually show an increase in their absolute size. Conversely, hypoallometric red domains, which should show the least areal contraction with reducing SV and TV, are actually the subcortical regions that show the greatest areal loss with mounting sex-chromosome dose. Thus, allometric analysis indicates that SCA actively "erases" the regional growth patterns that regulate normative relationships between striato-thalamic shape and brain size.

Although our study analyzes the normative allometry of subcortical shape using a parcellation defined by SCA effects, these analyses yield insights into the organization of subcortical shape in health. First, they show that the striatum and thalamus change their shape with increasing size, while the pallidum does not. With increasing nucleus size, the caudate body/tail and the dorsal thalamus become proportionately larger, whereas the putamen and lateroventral facets of the thalamus become proportionately smaller. Size-related variations in subcortical shape point toward local differences in the regulation of subcortical growth. A priority for future work will be testing whether regional differences in subcortical allometry correspond to candidate anatomical (e.g., proximity of hyperallometric regions to fluid-filled ventricles; Duvernoy, 1999), and/or connectivity-based (e.g., a topographical mirroring in the subcortex of regional differences in cortical expansion; Hill et al., 2010) regulators of subcortical growth.

Our analyses of normative subcortical allometry hint that sex could potentially influence normative relationships between TBV and shape; e.g., cyan and red domains of the thalamus show allometric scaling with thalamic size in females (hyper- and hypoallometric, respectively) but isometric scaling in males. Confirming the existence of such sexually distinct investments in regional brain growth in humans, would carry potential functional and/or clinical implications (Cahill, 2006), and recommend new analytic approaches for identifying sex-differences in human brain organization. Replication of these allometric analyses in large longitudinal samples will be needed to test whether Tanner stage and/or chronological age influence normative scaling within the brain. Delineating, and potentially dissociating, the effects of Tanner stage and chronological age has significant theoretical and methodological consequences. For example, if Tanner stage were found to exert age-independent effects on brain shape, then future developmental neuroimaging studies would require methodologies that can factor-out, or explicitly model the effects of pubertal progression.

**Limitations and future directions**

Our findings should be considered in light of certain study limitations. First, our cross-sectional study cannot model how age might alter sex, sex-chromosome dosage, and TBV effects on subcortical anatomy. The rarity of SCAs is a challenge for accrual of cohorts needed for longitudinal analyses. Second, it will be important to assess in future work whether gonadal steroids contribute to regional variation in male–female scaling differences

(e.g., via regional accentuations in sex-steroid biosynthesis such as those reported in the medial dorsal thalamic nucleus; Biegon et al., 2010). Third, the cellular bases for our neuroimaging results remain unclear. Given the divergent gene content of human X- and Y-chromosomes, convergent supernumerary X- and Y-chromosome effects on subcortical anatomy must reflect: (1) increased dose of homologous X–Y gene pairs (Otto et al., 2011; Bellott et al., 2014), or (2) increased nuclear chromatin dosage. Direct gene-expression studies will be required to test these hypotheses and the degree to which sex-chromosome dosage variation in aneuploidy fully recapitulates the effects of varying sex-chromosome dosage between karyotypically normal males and females. Fourth, future studies will be required to test whether the focal variations in subcortical anatomy that we link to sex, sex-chromosome dosage, and normative variation in brain size are associated with cognitive–behavioral variations.

These limitations notwithstanding, our study: (1) provides a refined understanding of normative sex-differences in human subcortical organization, (2) identifies subcortical systems distinctly vulnerable to SCA, and (3) demonstrates the necessity of considering normative allometry when evaluating neuroanatomy in health and disease.

## References


Ad-Dab'bagh Y, Einarson D, Lyttelton O, Muehlboeck S, Mok K, Ivanov O, Vincent R, Lepage C, Lerch J, Fombonne E, Evans A (2006) The CIVET image-processing environment: a fully automated comprehensive pipeline for anatomical neuroimaging research. Proceedings of the 12th Annual Meeting of the Human Brain Mapping Organization. Florence, Italy.

Ahsan RL, Allom R, Gousias IS, Habib H, Turkheimer FE, Free S, Lemieux L, Myers R, Duncan JS, Brooks DJ, Koepp MJ, Hammers A (2007) Volumes, spatial extents and a probabilistic atlas of the human basal ganglia and thalamus. Neuroimage 38:261–270. CrossRef Medline

Bellott DW, Hughes JF, Skaletsky H, Brown LG, Pyntikova T, Cho TJ, Koutseva N, Zaghlul S, Graves T, Rock S, Kremitzki C, Fulton RS, Dugan S, Ding Y, Morton D, Khan Z, Lewis L, Buhay C, Wang Q, Watt J, et al. (2014) Mammalian Y chromosomes retain widely expressed dosage-sensitive regulators. Nature 508:494–499. CrossRef Medline

Biegon A, Kim SW, Alexoff DL, Jayne M, Carter P, Hubbard B, King P, Logan J, Muench L, Pareto D, Schlyer D, Shea C, Telang F, Wang GJ, Xu Y, Fowler JS (2010) Unique distribution of aromatase in the human brain: *in vivo* studies with PET and [*N*-methyl-11C]vorozole. Synapse 64: 801–807. CrossRef Medline

Blumenthal JD, Baker EH, Lee NR, Wade B, Clasen LS, Lenroot RK, Giedd JN (2013) Brain morphological abnormalities in 49, XXXXY syndrome: a pediatric magnetic resonance imaging study. Neuroimage Clin 2: 197–203. CrossRef Medline

Bradshaw JL, Sheppard DM (2000) The neurodevelopmental frontostriatal disorders: evolutionary adaptiveness and anomalous lateralization. Brain Lang 73:297–320. CrossRef Medline

Brain Development Cooperative Group (2012) Total and regional brain volumes in a population-based normative sample from 4 to 18 years: the NIH MRI study of normal brain development. Cereb Cortex 22:1–12. CrossRef Medline

Bryant DM, Hoeft F, Lai S, Lackey J, Roeltgen D, Ross J, Reiss AL (2011) Neuroanatomical phenotype of Klinefelter syndrome in childhood: a voxel-based morphometry study. J Neurosci 31:6654–6660. CrossRef Medline

Bryant DM, Hoeft F, Lai S, Lackey J, Roeltgen D, Ross J, Reiss AL (2012) Sex chromosomes and the brain: a study of neuroanatomy in XYY syndrome: neuroanatomical variation in XYY syndrome. Dev Med Child Neurol 54:1149–1156. CrossRef Medline

Cahill L (2006) Why sex matters for neuroscience. Nat Rev Neurosci 7: 477–484. CrossRef Medline

Chakravarty MM, Bertrand G, Hodge CP, Sadikot AF, Collins DL (2006) The creation of a brain atlas for image guided neurosurgery using serial histological data. Neuroimage 30:359–376. CrossRef Medline

Chakravarty MM, Steadman P, van Eede MC, Calcott RD, Gu V, Shaw P, Raznahan A, Collins DL, Lerch JP (2013) Performing label-fusion-based segmentation using multiple automatically generated templates: MAGeT brain: label fusion segmentation using automatically generated templates. Hum Brain Mapp 34:2635–2654. CrossRef Medline

Choi EY, Yeo BT, Buckner RL (2012) The organization of the human striatum estimated by intrinsic functional connectivity. J Neurophysiol 108: 2242–2263. CrossRef Medline

Corre C, Friedel M, Vousden DA, Metcalf A, Spring S, Qiu LR, Lerch JP, Palmert MR (2014) Separate effects of sex hormones and sex chromosomes on brain structure and function revealed by high-resolution magnetic resonance imaging and spatial navigation assessment of the Four Core Genotype mouse model. Brain Struct Funct. Advance online publication. CrossRef Medline

Draganski B, Kherif F, Klöppel S, Cook PA, Alexander DC, Parker GJ, Deichmann R, Ashburner J, Frackowiak RS (2008) Evidence for segregated and integrative connectivity patterns in the human basal ganglia. J Neurosci 28:7143–7152. CrossRef Medline

Duvernoy HM (1999) The human brain. Vienna: Springer.

Escorial S, Román FJ, Martínez K, Burgaleta M, Karama S, Colom R (2015) Sex differences in neocortical structure and cognitive performance: a surface-based morphometry study. Neuroimage 104:355–365. CrossRef Medline

Finlay BL, Darlington RB (1995) Linked regularities in the development and evolution of mammalian brains. Science 268:1578–1584. CrossRef Medline

Genovese CR, Lazar NA, Nichols T (2002) Thresholding of statistical maps in functional neuroimaging using the false discovery rate. Neuroimage 15:870–878. CrossRef Medline

Giedd JN, Raznahan A, Alexander-Bloch A, Schmitt E, Gogtay N, Rapoport JL (2015) Child psychiatry branch of the national institute of mental health longitudinal structural magnetic resonance imaging study of human brain development. Neuropsychopharmacology 40:43–49. CrossRef Medline

Grahn JA, Parkinson JA, Owen AM (2008) The cognitive functions of the caudate nucleus. Prog Neurobiol 86:141–155. CrossRef Medline

Greene DJ, Laumann TO, Dubis JW, Ihnen SK, Neta M, Power JD, Pruett JR Jr, Black KJ, Schlaggar BL (2014) Developmental changes in the organization of functional connections between the basal ganglia and cerebral cortex. J Neurosci 34:5842–5854. CrossRef Medline

Hill J, Inder T, Neil J, Dierker D, Harwell J, Van Essen D (2010) Similar patterns of cortical expansion during human development and evolution. Proc Natl Acad Sci U S A 107:13135–13140. CrossRef Medline

Hong DS, Reiss AL (2014) Cognitive and neurological aspects of sex chromosome aneuploidies. Lancet Neurol 13:306–318. CrossRef Medline

Hong DS, Hoeft F, Marzelli MJ, Lepage JF, Roeltgen D, Ross J, Reiss AL (2014) Influence of the X-chromosome on neuroanatomy: evidence from turner and Klinefelter syndromes. J Neurosci 34:3509–3516. CrossRef Medline

Hughes JF, Rozen S (2012) Genomics and genetics of human and primate y chromosomes. Annu Rev Genomics Hum Genet 13:83–108. CrossRef Medline

Johnston MV (2001) Excitotoxicity in neonatal hypoxia. Ment Retard Dev Disabil Res Rev 7:229–234. CrossRef Medline

Kim DJ, Park B, Park HJ (2013) Functional connectivity-based identification of subdivisions of the basal ganglia and thalamus using multilevel independent component analysis of resting state fMRI. Hum Brain Mapp 34:1371–1385. CrossRef Medline

Lee NR, Wallace GL, Adeyemi EI, Lopez KC, Blumenthal JD, Clasen LS, Giedd JN (2012) Dosage effects of X and Y chromosomes on language and social functioning in children with supernumerary sex chromosome aneuploidies: implications for idiopathic language impairment and autism spectrum disorders. J Child Psychol Psychiatry 53:1072–1081. CrossRef Medline

Lentini E, Kasahara M, Arver S, Savic I (2013) Sex differences in the human brain and the impact of sex chromosomes and sex hormones. Cereb Cortex 23:2322–2336. CrossRef Medline

Meltzer H, Gatward R, Goodman R, Ford T (2003) The mental health of children and adolescents in Great Britain: summary report. Int Rev Psychiatry 15:185–187. CrossRef Medline

Ostby Y, Tamnes CK, Fjell AM, Westlye LT, Due-Tønnessen P, Walhovd KB (2009) Heterogeneity in subcortical brain development: a structural magnetic resonance imaging study of brain maturation from 8 to 30 years. J Neurosci 29:11772–11782. CrossRef Medline

Otto SP, Pannell JR, Peichel CL, Ashman TL, Charlesworth D, Chippindale AK, Delph LF, Guerrero RF, Scarpino SV, McAllister BF (2011) About PAR: the distinct evolutionary dynamics of the pseudoautosomal region. Trends Genet 27:358–367. CrossRef Medline

Raznahan A, Lee Y, Stidd R, Long R, Greenstein D, Clasen L, Addington A, Gogtay N, Rapoport JL, Giedd JN (2010) Longitudinally mapping the influence of sex and androgen signaling on the dynamics of human cortical maturation in adolescence. Proc Natl Acad Sci U S A 107: 16988–16993. CrossRef Medline

Raznahan A, Shaw PW, Lerch JP, Clasen LS, Greenstein D, Berman R, Pipitone J, Chakravarty MM, Giedd JN (2014) Longitudinal four-dimensional mapping of subcortical anatomy in human development. Proc Natl Acad Sci U S A 111:1592–1597. CrossRef Medline

Raznahan A, Lue Y, Probst F, Greenstein D, Giedd J, Wang C, Lerch J, Swerdloff R (2015) Triangulating the sexually dimorphic brain through high-resolution neuroimaging of murine sex chromosome aneuploidies. Brain Struct Funct 220:3581–3593. CrossRef Medline

Raznahan A, Lee NR, Greenstein D, Wallace GL, Blumenthal JD, Clasen LS, Giedd JN (2016) Globally divergent but locally convergent X- and Y-chromosome influences on cortical development. Cereb Cortex 26: 70–79. CrossRef Medline

Rijpkema M, Everaerd D, van der Pol C, Franke B, Tendolkar I, Fernández G (2012) Normal sexual dimorphism in the human basal ganglia. Hum Brain Mapp 33:1246–1252. CrossRef Medline

Roalf DR, Gur RE, Ruparel K, Calkins ME, Satterthwaite TD, Bilker WB, Hakonarson H, Harris LJ, Gur RC (2014) Within-individual variability in neurocognitive performance: age- and sex-related differences in children and youths from ages 8 to 21. Neuropsychology 28:506–518. CrossRef Medline

Rutter M, Caspi A, Moffitt TE (2003) Using sex differences in psychopathology to study causal mechanisms: unifying issues and research strategies [Review]. J Child Psychol Psychiatry 44:1092–1115. CrossRef Medline

Sheltzer JM, Torres EM, Dunham MJ, Amon A (2012) Transcriptional consequences of aneuploidy. Proc Natl Acad Sci U S A 109:12644–12649. CrossRef Medline

Sowell ER, Trauner DA, Gamst A, Jernigan TL (2002) Development of cortical and subcortical brain structures in childhood and adolescence: a structural MRI study. Dev Med Child Neurol 44:4–16. CrossRef Medline

Tartaglia N, Davis S, Hench A, Nimishakavi S, Beauregard R, Reynolds A, Fenton L, Albrecht L, Ross J, Visootsak J, Hansen R, Hagerman R (2008) A new look at XXYY syndrome: medical and psychological features. Am J Med Genet A 146A:1509–1522. CrossRef Medline

Toro R, Chupin M, Garnero L, Leonard G, Perron M, Pike B, Pitiot A, Richer L, Veillette S, Pausova Z, Paus T (2009) Brain volumes and Val66Met polymorphism of the BDNF gene: local or global effects? Brain Struct Funct 213:501–509. CrossRef Medline

Voorn P, Vanderschuren LJ, Groenewegen HJ, Robbins TW, Pennartz CM (2004) Putting a spin on the dorsal-ventral divide of the striatum. Trends Neurosci 27:468–474. CrossRef Medline

Wierenga L, Langen M, Ambrosino S, van Dijk S, Oranje B, Durston S (2014) Typical development of basal ganglia, hippocampus, amygdala and cerebellum from age 7 to 24. Neuroimage 96:67–72. CrossRef Medline